Proceedings of the 21st ICSMGE, Vienna, Austria, 14 – 19 June 2026. Pistrol, Adam & Schweiger (eds.)
Published by: ÖGG, Austrian Society for Geomechanics, Salzburg, Austria, ISBN 978-3-9503898-4-5
https://doi.org/10.53243/ICSMGE2026-2315

Study on seismic characteristics of frame structures supported by foundation combined with soil bags, piles and footings

Tatsuya Doi
Center for Railway Earthquake Engineering Research, Railway Technical Research Institute, Japan,
doi.tatsuya.45@rtri.or.jp

Shota Nomoto
Tokyo Metropolitan Area Construction Project Management Office, East Japan Railway Company, Japan

ABSTRACT: One of the authors has been developing a new foundation combined with soil bags, piles and footings. The purpose of developing this foundation is to reduce bending moment of piers by cutting off fixed connections between piles and a footing and decreasing response acceleration of piers. When the proposed foundation is applied to frame structures such as station buildings above railway tracks, however, seismic response is quite different from that of piers. In this study, therefore, an analytical method that can reproduce the seismic response of frame structures with the proposed foundations is developed by conducting reduced-scale shake table tests and their reproducing analysis. Next, the seismic response of the proposed foundation is compared with that of the pile foundation through numerical experiments on full-scale frame structures with proposed foundation and conventional pile foundation, and the effect of introducing the proposed foundation was discussed. Through the reduced-scale shake table tests and their reproducing analysis, it was found that the constructed analytical model was able to evaluate the test results on the safer side, although it was not able to reproduce the test results completely. Furthermore, numerical experiments on full-scale structures using the constructed analytical method showed that the response acceleration of the frame structures with the proposed foundation is smaller than that with the pile foundation because the natural period of the proposed foundation becomes longer than the dominant period of the acceleration on ground surface, and correspondingly, the damage to the columns is also suppressed. It was also found that dynamic displacement at the upper slab was suppressed in the proposed foundation compared to the pile foundation, mainly due to the suppression of deformation from the deeper part of the foundation.

KEYWORDS: Pile, soil bag, frame structure.

1 INTRODUCTION

When constructing frame structures such as station buildings above railway tracks in urban areas, it is often necessary to use caisson type piles as foundations due to existing buried obstacles. The construction of these caisson type piles requires great effort. Therefore, a method of using micropiles that can be driven through the buried obstacles is being considered. However, there is concern that the joint structures between the pile heads and the footings will become complicated. On the other hand, one of the authors have been developing a new composite foundation composed of piles and soil bags (Doi et al., 2020a; Doi et al., 2022) as shown in Figure 1 (hereinafter referred to as the "proposed foundation"). When the proposed foundation is applied to bridge piers, the bending moment and response acceleration of the piers can be reduced by the rocking of the piers during earthquakes due to the insulation between the piles and footings, and the stress concentration on the edge piles can be mitigated by the installation of soil bags (Doi et al., 2022). When the proposed foundation is applied to station buildings above railway tracks as shown in Figure 2, the pile-head joint structures can be eliminated, and it is expected that the constructability will be improved. It is important to understand the seismic response characteristics of station buildings with the proposed foundation because station buildings above railway tracks are usually frame structures without footing beams, and their seismic response is significantly different from that of bridge piers.

There are many experimental and analytical studies of frame structures supported by spread foundation without footing beams. For example, Chang et al. (2007) verified the effect of shear walls in reinforcing frame structures in a model experiment in a 20g centrifugal force field. Gelagoti et al. (2012) showed by 3D dynamic elastoplastic FEM analysis that seismic energy can be effectively dissipated by setting the bearing capacity of the foundation and columns in good balance while allowing rocking. On the other hand, there are no examples of frame structures without footing beams in which the piles and footings are insulated, or in which piles and soil bags are used in combination. In this study, therefore, an analytical method that can reproduce the experimental results is developed by conducting reduced-size model shake table tests of a frame structure with the proposed foundation type and its reproducing analysis. Next, the seismic response of the proposed foundation is compared with that of a pile foundation through numerical experiments on a full-scale structure using the developed analytical method and discuss the effect of introducing the proposed foundation.

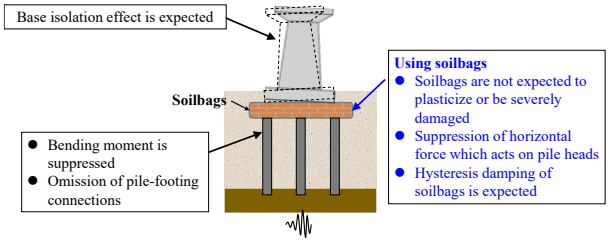

Figure 1. Overview of the proposed foundation (Doi et al., 2022).

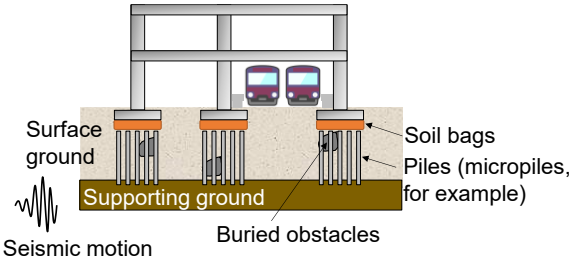

Figure 2. Image of station building above railway tracks with proposed foundation.

2 SCALED SHAKE TABLE TESTS AND THEIR REPRODUCING ANALYSIS

2.1 *Outline of shake table tests*

A fixed soil vessel was used for the shake table tests. The size of the soil vessel was 2 m in length, 0.6 m in width, and 1.4 m in height (internal dimensions). The dimensions of the models are based on the transverse direction of the design example of a station building above railway tracks (Railway Technical Research Institute, 2009) shown in Figure 3.

Figure 4 shows an outline of the test specimen and layout of measurement sensors. Weights of 19.4 kg and 48.5 kg were placed in the upper and lower slabs of the model, respectively. The supporting ground consisted of M40 crushed stone with degree of compaction of 90%, and the surface ground consisted of Tohoku silica sand No. 6 with relative density of 80%. High-density polyethylene net was used for the model bag, and Kashima silica sand No. 2 was used as filling material of model soil bags. The density of the filling material was 1.625 g/cm^3 in the air-dried state. Six sheets of sandpaper (#80) were stuck on the underside of each model footing of the station building with the proposed foundation to ensure friction with the soil bags. The friction angle among the soil bags and between the soil bags and the underside of the footings were confirmed by friction tests, and friction angles of 21.7° and 48.7° were obtained, respectively. The upper and lower columns were square steel columns of 10 mm x 10 mm and 20 mm x 20 mm, respectively. The slabs were steel plates with a thickness of 4.5 mm for the upper slab and 9 mm for the lower slab. The micropile models were made of acrylic pipes with diameter of 15 mm and thickness of 3 mm. The deformation coefficient of the acrylic pipe is 3767 N/mm^2 based on the bending tests. The thickness of the micropiles were selected so that the product of the pile characteristic value β and the pile length l, βl, would be equivalent to that of the actual pile.

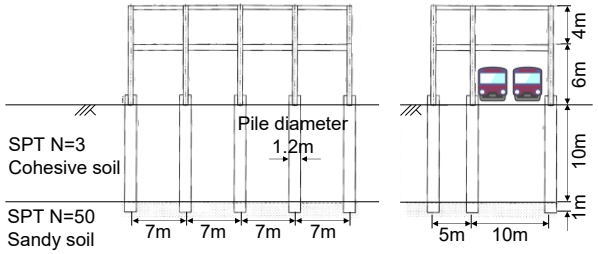

Figure 3. Outline of design example of station building above tracks (2-story building) (Railway Technical Research Institute, 2009).

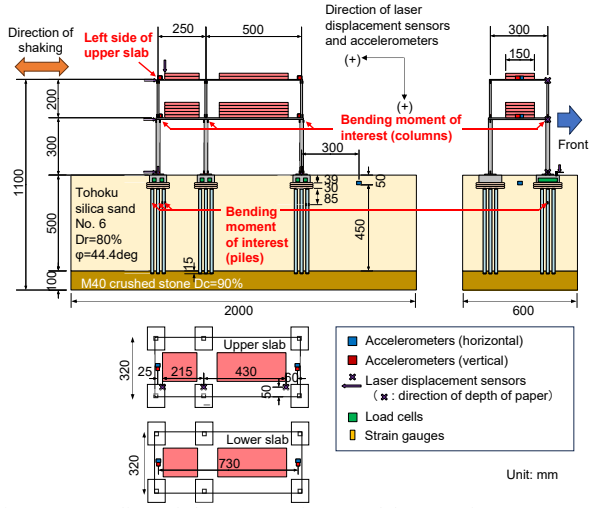

Figure 4. Outline of the test specimen and layout of measurement sensors.

During the shaking, the horizontal acceleration of the buildings and the ground, the horizontal displacement of the buildings, and the strain of the columns and piles were measured. The horizontal acceleration and displacement are positive in the left direction, and vertical acceleration and displacement are positive in the downward direction.

The input wave is Spectrum II (normal ground) shown in Figure 5 (Railway Technical Research Institute, 2012a), whose amplitude was adjusted to 900 cm/s^2 and time axis was compressed by a factor of $1/\sqrt{20}$ according to the similarity laws.

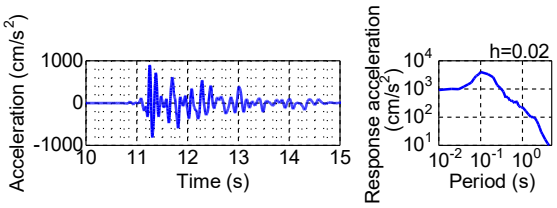

Figure 5. Input wave for shake table tests.

2.2 *Outline of reproducing analysis*

The analytical model was a two-dimensional beam-spring system model. Figure 6 shows an outline of the reproducing analysis model. In the shake table tests, there are two rows of columns and footings in the width direction, however, the front row was modelled in the reproducing analysis by assuming uniform behaviour in the width direction. Correspondingly, the nodal masses were set to half the value of the model building. In the tests, the strain of the columns was within the yield strain, and no significant damage was observed in the slabs and piles. Therefore, the influence of plasticity on the columns, slabs, and piles was considered to be small in the tests, and they were modelled using linear beam elements. Rigid beam elements were installed on each pile head to consider the width of the piles.

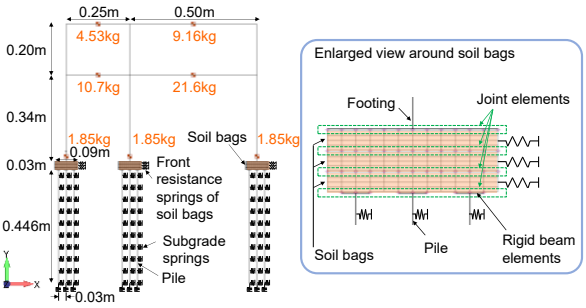

Figure 6. Outline of reproducing analysis model.

In a previous study (Doi et al., 2020a), soil bags were modelled as linear elastic elements with their deformation coefficient of 21000 kN/m^2 for 1 m in width. Since the width of the footing is 120 mm in the present model building, the deformation coefficient of the soil bags was set to 21000 kN/m^2 × 120 mm / 1000 mm = 2520 kN/m^2. The front resistance of the soil bags was modelled with bilinear springs, whose nonlinearity was set based on design standards for railway structures and commentary (Foundation structures) (Railway Technical Research Institute, 2012b). The horizontal soil spring of the pile shaft was modelled using bilinear springs according to design standards for railway structures and commentary (Foundation structures) (Railway Technical Research Institute, 2012b). The vertical spring at the pile tip was assumed to be linear because the effect of support yielding at the pile tip is considered to be small. The vertical shear spring at the pile shaft was ignored because the vertical spring at the pile tip is linear and the

influence of the vertical shear resistance of the pile shaft is small.

Joint elements were placed between footings and soil bags, and among soil bags. The parameters of the joint elements are shown in Figure 7. The cohesion and friction angle of the joint elements were set based on the above-mentioned friction tests. The initial stiffness of the joint elements was set so that the joint elements were sufficiently rigid compared to the soil bags, based on the mesh interval and the stiffness of the soil bags. The rate of stiffness reduction was set to be as small as possible to the extent that the analysis is stable.

Numerical integration for the dynamic analysis was performed using the Newmark-β method (β=1/4). The integration interval was set to 0.0005 s, which is sufficiently small value to ensure stability of the calculation. The damping matrix was set using element Rayleigh damping, where damping of joint elements was set to zero to prevent excessive damping in elements with large initial stiffness, and Rayleigh damping was applied to other elements. The constants of Rayleigh damping were set so that the damping constants are 2% (based on the response factor of the first-order peak of the transfer function of the test specimen obtained from white noise shaking conducted separately) at 20 Hz and the first natural frequency of the structure (13 Hz).

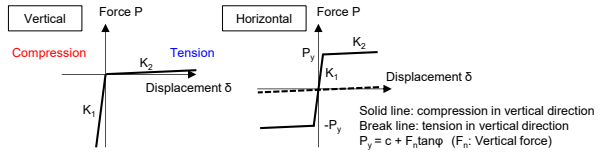

	Between soil bags and footing		Among soil bags, between soil bags and piles	
	Vertical direction	Horizontal direction	Vertical direction	Horizontal direction
K_1 (kN/m)	1.0×10^4	1.0×10^4	1.0×10^4	1.0×10^4
K_2 (kN/m)	50.0	0.01	50.0	0.01
c (kN/m^2)	-	0.01	-	0.01
φ (deg.)	-	48.7	-	21.7

Figure 7. Parameters of joint elements.

2.3 *Comparison between tests and analysis*

A comparison of the response horizontal acceleration and acceleration response spectra at the left end of the upper slab is shown in Figure 8, and a comparison of the horizontal response displacement is shown in Figure 9. The maximum response acceleration of the analysis is approximately 1.7 times as large as that of the tests. The acceleration response spectra on the lower side of Figure 8 shows that the response acceleration of the analysis is larger than that of the tests on the short period, and thus, the maximum response acceleration of the analysis is larger mainly due to this short period component. This is due to the pulsed response caused by the detachment and re-contact of the joint elements. However, when focusing on the first-order natural period of the station building model (1/13 = 0.077s), the response acceleration is almost the same. Figure 9 shows that the maximum response displacement of the analysis is equivalent to that of the tests. However, the trend of response displacement after around 11.75 s is not fully explained. This is because the excitation in the tests caused displacement between the soil bags and between the soil bags and footings, and disturbance in the ground in front of the soil bags, which have resulted in differences from the conditions assumed for the joint elements and the resistance springs in front of the soil bags shown in Figure 7.

Figure 10 compares the bending moment time histories at the top of the lower columns (see Figure 4), where the bending moment is larger. The bending moment in Figure 10 is shown with the direction of bending tension on the right side of the columns as positive. The analytical bending moment is generally equivalent to the test results, although the analytical result is slightly larger than the test results in the left column. Figure 11 shows a comparison of the bending moment time histories of the piles immediately below the left footing (see Figure 4). The bending moment in Figure 11 is shown with the direction of bending tension on the right side of the piles as positive. The analytical results are larger than the test results, especially for the left pile. This is because all the horizontal forces from the underside of the soil bags act on the pile heads in the analysis because the analysis neglects the influence of the ground between the piles, whereas the ground between the piles also shares the horizontal forces in the shake table tests.

As described above, although the constructed analytical model does not fully reproduce the test results, it is able to evaluate the test results on the safer side. In the next section, numerical experiments will be conducted on a full-scale structure using the developed analytical method.

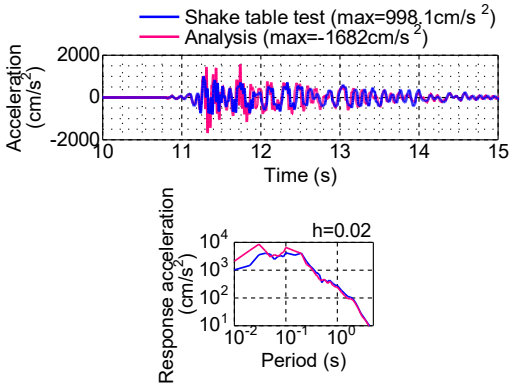

Figure 8. Comparison of the response horizontal acceleration and acceleration response spectra at the left end of the upper slab.

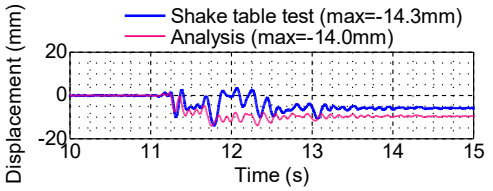

Figure 9. Comparison of the horizontal response displacement.

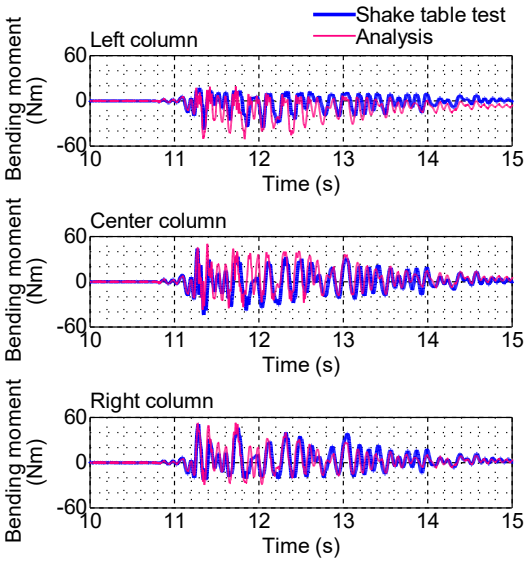

Figure 10. Comparison of bending moment of columns.

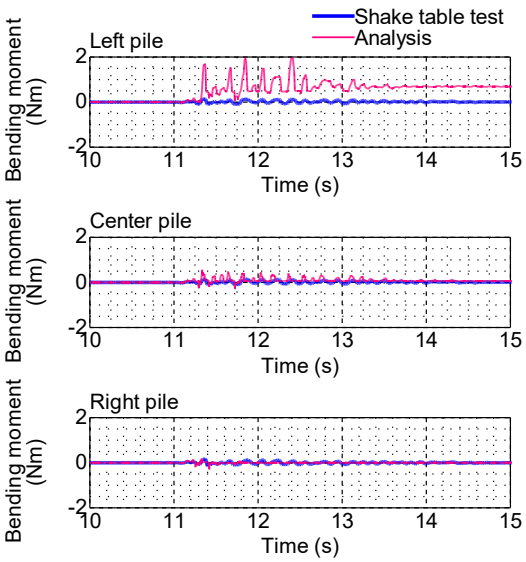

Figure 11. Comparison of bending moment of piles.

3 NUMERICAL EXPERIMENTS ON FULL-SCALE STRUCTURES

3.1 *Outline of analysis model*

Figure 12 shows the specifications of the structure examined in this study. The structure examined in this study is a station building shown in Figure 3, in which its foundation has been replaced from the conventional pile foundation to the proposed foundation. The specifications of the columns and beams have been modified as shown in Figure 12(a). As shown in Figure 3, the ground consists of a surface layer (clay with SPT-N value of 3 and thickness of 10 m) and a load bearing layer (sandy soil with SPT-*N* value of 50). The first-order natural period of the target ground is 0.28 s. Steel pipe piles with a length of 11 m, a diameter of 300 mm, and a thickness of 12 mm were used. To prevent punching failure of the soil bags, steel plates were installed at each pile head as shown in Figure 12(b). The soil bags have dimensions of 300 mm in width, 300 mm in depth, and 100 mm in height and are composed of M30 granulated crushed stone (degree of compaction is approximately 95%) and geotextile (KJV-60W). The soil bags were stacked in three layers, and the geotextile was used to integrate the entire layers from the outside to prevent sliding between the soil bags.

Figure 13 shows an overview of the 3D response value calculation model of the proposed foundation developed based on the method developed in Chapter 2. The response values were calculated using a free field-structure integrated dynamic analysis model. The nonlinearity of the free field was modelled using GHE-S model (Railway Technical Research Institute, 2012a). Columns and piles were modelled with beam elements. Sufficiently rigid plate elements were introduced at each pile head to model the contact area between the soil bags and the pile head. Ground resistance of the piles and in front of footings and soil bags was modelled by bilinear spring elements based on the design standard (Railway Technical Research Institute, 2012b). It should be noted that, as for vertical ground resistance of the piles, only vertical resistance at the pile tip was considered, and the vertical resistance at the pile shaft was neglected. The soil bags were modeled as linear elastic solid elements. Their deformation coefficients were set from an analysis of the compression of a single soil bag used in this study, using the same method as that used in a reproduction analysis of a previous compression test of a single soil bag (Doi et al., 2020b). Specifically, the stiffness was set to 35280 kN/m^2, which is the secant stiffness at the point where 65% of the vertical strain when compressive failure of the soil bag occurs against large scale earthquake (L2 earthquake motion defined in Japanese design standard (Railway Technical Research Institute, 2012a)). Compressive failure is defined as the point at which the geotextile tension reaches the tensile capacity 86 kN/m against L2 earthquake. Sliding between the soil bags was neglected under the assumption that the soil bags were integrated with each other from the outside. The contact and separation between the soil bags and pile heads and between the soil bags and footings were modelled using joint elements. The friction angle and adhesion of joint elements were set to 28.9° (coefficient of friction 0.552) and 2.1 kN/m^2, respectively, based on the results of friction tests conducted separately. The initial stiffness was set to be 1.0×10^7 kN/m^2 per pile head with a stiffness reduction ratio of 0.005.

The pile foundations were modelled as cast-in-place piles with a pile diameter of 1.2 m as shown in Figure 3.

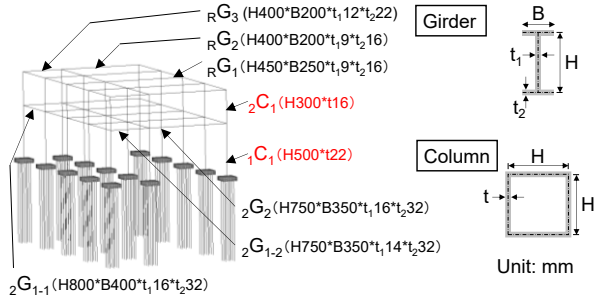

(a) Specifications of columns and beams

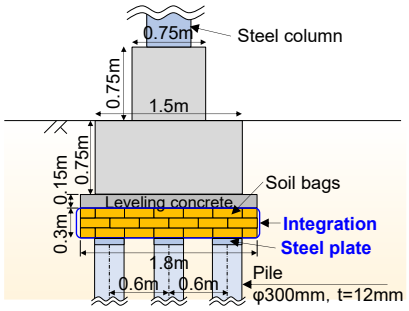

(b) Specifications of foundations

Figure 12. Specifications of the structure examined in this study.

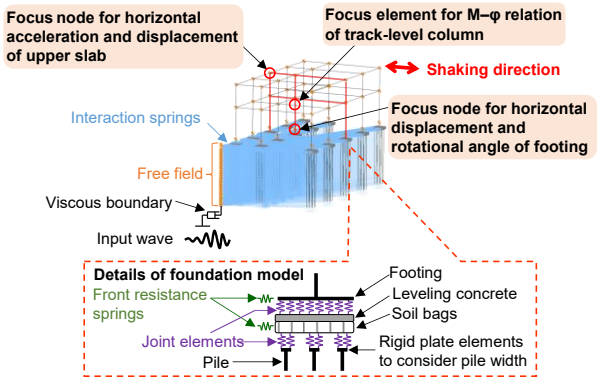

Figure 13. 3D response value calculation model of the proposed foundation.

3.2 *Analysis conditions*

The input motion was the spectrum II motion (defined on bedrock) shown in Figure 14, within the period range of 6 s to 30 s. The input motion was applied in the direction perpendicular to the railway tracks from the viscous boundary at the bottom of the free-field model. Numerical integration was

performed using the Newmark-β method (β=1/4) with a time interval of 0.002 s. The damping matrix was set by Rayleigh element damping, where the damping of joint elements was set to zero and the damping of other elements was given by Rayleigh damping for the proposed foundation and Rayleigh damping for the pile foundation. Rayleigh damping was set so that the damping ratio would be 3% at both fundamental frequency of the free-field ground (3.6 Hz) and 10 Hz.

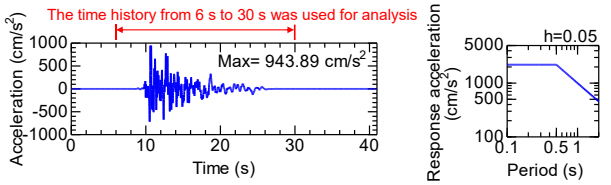

Figure 14. Input earthquake motion (defined on engineering bed rock for seismic design).

3.3 *Comparison of seismic response between proposed foundation and conventional pile foundation*

3.3.1 *Building*

Firstly, the natural period of the building is discussed. The results of the eigenvalue analysis are shown in Table 1. The natural period of the proposed foundation is slightly longer than that of the pile foundation in the first-order mode (structure). Since the specifications of columns and beams are the same for the proposed foundation and the pile foundation, the difference in the natural period is due to the difference in stiffness of the entire structural system caused by the difference in foundation type. The response acceleration at the ground surface and the acceleration response spectrum are shown in Figure 15. The acceleration response spectrum of the ground surface acceleration is dominant around 0.5 s to 0.8 s, which is around the first-order natural period of the proposed foundation and pile foundation shown in Table 1.

Table 1. Results of eigenvalue analysis.

Mode	Proposed foundation		Pile foundation	
	Natural period (s)	Effective mass ratio	Natural period (s)	Effective mass ratio
1st (structure)	0.776	0.761	0.645	0.549
2nd (structure)	0.576	0.0821	0.504	0.0540

Next, the dynamic response of the station building is discussed. The focus of the response is shown in Figure 13. The response acceleration time histories of the proposed foundation and the pile foundation at the upper slab are shown in Figure 16. The maximum response acceleration of the pile foundation is approximately 1.2 times that of the proposed foundation. The acceleration response spectrum of the ground surface acceleration in Figure 15 shows that the natural period of the proposed foundation in the elastic state is 0.776 s, and the response acceleration decreases due to the nonlinearization of the structural system. On the other hand, the natural period of the pile foundation in the elastic state is 0.645 s, and the response acceleration increases due to the nonlinearization of the structural system. This is the reason why the response acceleration of the pile foundation is larger than that of the proposed foundation. The response displacement time histories of the proposed foundation and pile foundation at the upper slab are shown in Figure 17. The response displacement of the pile foundation is larger than that of the proposed foundation. This is due to the difference in the type of foundation, which will be discussed later. Figure 18 shows the moment (M)-curvature (ϕ) relation for the track floor column. Corresponding to the response acceleration shown in Figure 16, the response curvature in the proposed foundation is smaller than that in the pile foundation. This suggests that damage to columns is more effectively suppressed in the proposed foundation than in the pile foundation.

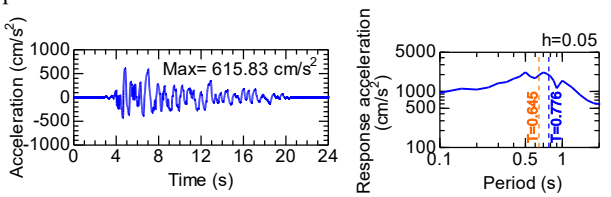

Figure 15. Response acceleration at the ground surface and the acceleration response spectrum.

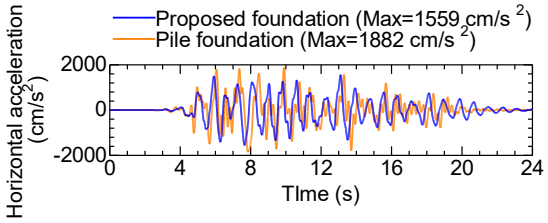

Figure 16. Horizontal response acceleration time histories at the upper slab.

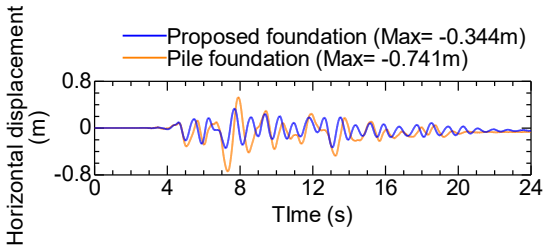

Figure 17. Horizontal response displacement time histories at the upper slab.

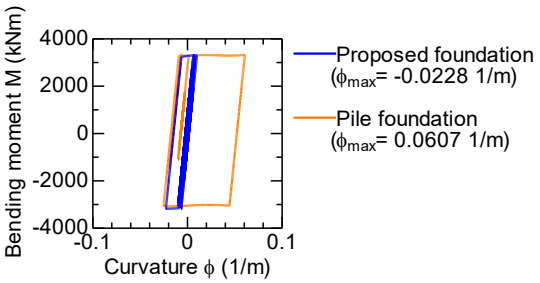

Figure 18. M-ϕ relation of the track-level column.

3.3.2 *Foundation*

The dynamic response of the foundation will be discussed. The focus of the response is shown in Figure 13. Figure 19 shows the horizontal displacement at the footing of the proposed foundation and at the pile head of the pile foundation (relative to the ground surface displacement). Figure 20 shows the rotational angle at the footing of the proposed foundation and at the pile head of the pile foundation. The maximum horizontal displacement of the pile foundation is approximately 8.8 times that of the proposed foundation, and the maximum rotational angle of the pile foundation is approximately 1.3 times that of the proposed foundation. One of the reasons for this difference is the difference in response acceleration discussed in Figure 16. Furthermore, as shown in the deformation distributions at the time of maximum rotational angle in Figure 21, horizontal force acts on the pile head directly in the pile foundation, causing bending deformation from the deeper parts of the ground. This leads to larger horizontal displacement and rotational angle at the pile heads compared to the proposed foundation. Additionally, in the proposed foundation, the resistance in front of the soil bags and footings is considered,

which helps to suppress the horizontal force transmitted to the pile heads, and this also contributes to the difference in the horizontal displacement and rotational angle.

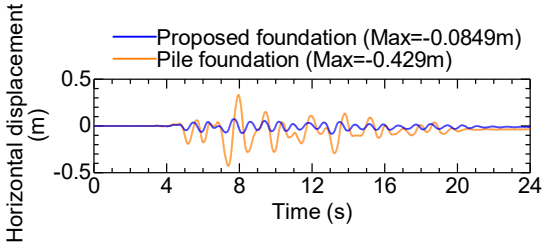

Figure 19. Horizontal displacement at the footing of the proposed foundation and at the pile head of the pile foundation.

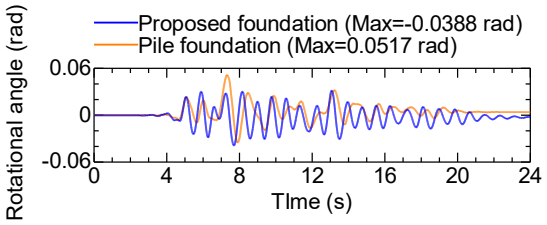

Figure 20. Rotational angle at the footing of the proposed foundation and at the pile head of the pile foundation.

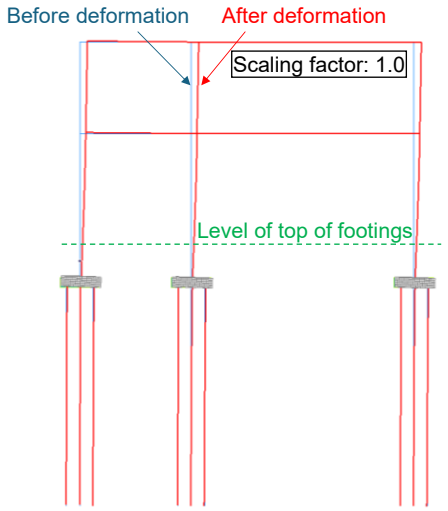

(a) Proposed foundation (t = 7.688 s)

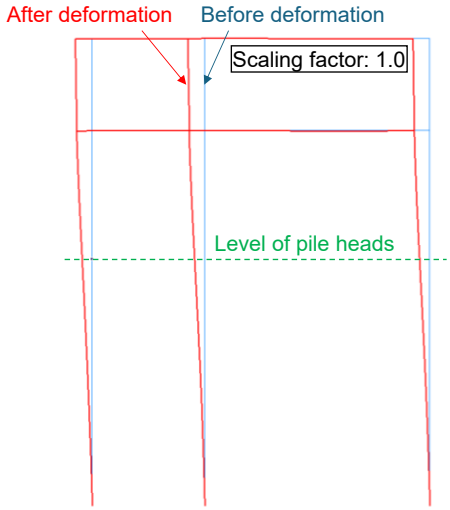

(b) Pile foundation (t = 7.32 s)

Figure 21. Deformation distributions at the row containing the focus elements in Figure 13 at the time when rotational angle is maximum.

4 CONCLUSIONS

In this study, the applicability of a new foundation system combined with soil bags, piles and footings for station buildings above railway tracks was examined through the development of an analytical method and numerical experiments on full-scale structures. First, reduced-scale shake table tests of a frame structure using the proposed foundation and their reproducing analysis were conducted to develop an analytical method capable of reproducing the test results. Then, using the developed analytical method, numerical experiments were performed on full-scale structures to compare the seismic responses of the proposed foundation with those of conventional cast-in-place pile foundations. The effectiveness of introducing the proposed foundation was then discussed based on the results. The findings of this study are as follows:

(1) Although the analytical model cannot completely reproduce the results of the reduced model tests, the overall results can be evaluated on the safer side of the test results.

(2) The response acceleration of the full-scale structure using proposed foundation is smaller than that of the pile foundation because natural period of the structural system becomes longer, and correspondingly, the damage to the columns is suppressed.

(3) The dynamic displacement of the upper slab of the building with proposed foundation is suppressed mainly due to the suppression of deformation from the deeper part of the foundation compared to the pile foundation.

The findings can be used to introduce a foundation method that is easier to construct than conventional pile foundations and can reduce damage to structural members and dynamic displacement during earthquakes.

5 REFERENCES

Chang, B.J., Raychowdhury, P., Hutchinson, T.C., Thomas, J., Gajan, S., Kutter, B.L. 2007. Evaluation of the seismic performance of combined frame-wall-foundation structural systems through centrifuge testing, *Proc. 4th International Conference on Earthquake Geotechnical Engineering*, Thessaloniki, Paper No. 1497.

Doi, T., Yamada, S., Murono, Y., Cho, H. 2020a. Development of spread foundation composed of micropiles and soilbags to reduce seismic response of structures. *Quarterly Report of RTRI* 61, 215-221.

Doi, T., Murono, Y., Cho, H. 2020b. Model test and corresponding simulation on compressive characteristics of soilbags. *International Journal of Civil Infrastructure* 3, 41-47.

Doi, T., Murono, Y., Iwai, H., and Zhang, F. 2022. Numerical investigation on dynamic behavior of a composite foundation composed of soilbags and piles by 3D elastoplastic FEM, *Soils and Foundations* 62(3), 101158.

Gelagoti, F., Kourkoulis, R., Anastasopoulos, I. and Gazetas, G. 2012. Rocking isolation of low-rise frame structures founded on isolated footings, *Earthquake Engineering & Structural Dynamics*, 41, 1177-1197.

Railway Technical Research Institute 2009. *Structural design standard for buildings (low-rise) above railway tracks* (in Japanese).

Railway Technical Research Institute 2012a. *Design standards for railway structures and commentary (seismic design)*, Maruzen.

Railway Technical Research Institute 2012b. *Design standards for railway structures and commentary (foundation structures)*, Maruzen (in Japanese).